

# CAAP Quarterly Report

Date of Report: *February 28<sup>th</sup>, 2021*

Prepared for: *U.S. DOT Pipeline and Hazardous Materials Safety Administration*

Contract Number: *693JK31850007CAAP*

Project Title: *AI-enabled ILI robot with integrated structured light NDE for distribution pipelines*

Prepared by: *Mohand Alzuhiri, Zi Li, Jiaoyang Li, Preston Fairchild, Claudia Chen*

Contact Information: *Zaid Obeidi (Technical POC) and Zhongquan Zhou (AOR), Dr. Yiming Deng (MSU), Dr. Xiaobo Tan (MSU), and Dr. Hao Zhang (CSM)*

For quarterly period ending: *February 28<sup>th</sup>, 2021*

## **Business and Activity Section**

### **(a) Contract Activity**

**Project abstract:** Underground gas pipeline networks extend over 3 million miles in the United States of America. The aging of these infrastructures, combined with external damages from third-party excavation operations, is creating safety concerns for both operators and residents in the vicinity of these pipelines. In this proposal, we will collaborate with GTI/OTD and industry to develop an integrated AI-enabled robotic platform with a structured light-based NDE inspection tool for the scanning of medium density polyethylene (MDPE) pipes used in natural gas distribution. Unlike the direct optical inspection methods with cameras and light sources, the proposed tool will provide the operator with precise 3D information about the status of the pipe internal surface, which increases the probability of detection and leads to better damage evaluation capabilities. The tool will also provide an embedded electronic stabilization procedure to reduce the effect of vibration during the scanning process. The structured light sensor is mounted on a highly flexible snake robot that can carry the sensor and maneuver it through the complex gas pipeline networks. The AI-enabled shared control method combines autonomous decision support and high-level human commands to improve the safety and usability of robot control.

In this project, our multi-university team will build on our prior work sponsored by PHMSA, OTD, and DOE to enhance the capabilities of the scanning platform and improve the ease of operation, and foster the collaboration between the academic institution (MSU, CSM), research institution (GTI) and industry (OTD, utility companies). This will be achieved by addressing the lessons learned during the initial testing in the OTD roadmap project and the feedback from our industry partners. The main research objectives can be summarized as follows:

- Design and develop a structured light endoscopic sensor for the inspection of the pipe internal defects.
- Automate the scanning process to reduce the amount of expertise needed to perform the inspection and reconstruction process.
- Design and develop a flexible robotic platform to maneuver the sensor through the complex pipelines networks
- Implement a shared control method based on reinforcement learning to allow a user to control the robot more easily and safely.

Educational Objectives: Another major objective of the proposed effort is to inspire, educate and train Ph.D. and MS students to address pipeline safety challenges, potentially as a career after their graduation. If funded, three Ph.D. students from the three collaborating laboratories and several MS/undergraduate students will participate in

this CAAP program. They will be trained and educated in science and engineering to address the pipeline safety and integrity challenges. The PIs believe that education is a critical component of the CAAP project, and we will integrate research with educational activities to prepare the next-generation scientists and engineers for the gas and pipeline industry. Specific educational objectives include:

- Inspiring, educating, and training the graduate students at MSU and CSM as research assistants for pipe integrity assessment and management. Our previous successful CAAP projects have produced several engineers, researchers, and summer interns in the gas and pipeline industry,
- Integrating research topics from this effort with the existing undergraduate research programs at MSU, e.g. ENSURE program at MSU College of Engineering, and CSM, e.g., Mines Undergraduate Research Fellowship (MURF), to involve undergraduate students in pipe safety research.
- Improving the curriculum at MSU (e.g., Nondestructive Evaluation) and CSM (e.g., Artificial Intelligence and Human-Centered Robotics) using the scientific findings and achievement from the proposed research,
- Adapt research topics from this project to student projects in a seminar, senior design, and project courses, in order to make educational impacts on broader groups of students,
- Encourage the graduate research assistants involved in this project and students in the courses to apply for internships with USDOT/PHMSA and industry to practice their learned skills and gain practical experiences in areas related to pipeline safety and integrity.

The above-mentioned goals and objectives of this CAAP project will be well addressed and supported by the proposed research tasks. Development, demonstrations, and potential standardization to ensure the integrity of pipeline facilities will be carried out with the collaborative effort among two universities and our industry partner, Gas Technology Institution. The quality of the research results will be overseen by the PIs and the DOT program manager and submitted to high-profile and peer-reviewed journals and leading conferences. The proposed collaborative work provides an excellent environment for the integration of research and education as well as tremendous opportunities for two universities supported by this DOT CAAP funding mechanism. The graduate students supported by this CAAP research will be heavily exposed to ILI, NDE, reliability, and engineering design topics for emerging pipeline R&D technologies. The PIs have been actively encouraging students to participate in past and ongoing DOT projects and present papers at national and international conferences. Students who are not directly participating in the CAAP project will also benefit from the research findings through the undergraduate and graduate courses taught by the PIs and through attending university-wide research symposium and workshop.

### **(b) Status Update of Past Quarter Activities**

Below is a high-level summary of the activities performed during this quarter:

- MSU(NDEL):
  - Implemented the synchronized acquisition approach.
  - Developed a new projection module.
  - Started the work on the automated calibration algorithm.
- MSU(SML):
  - Design of miniaturized robotic platform.
- CSM (HRCL) :
  -

### **(c) Cost share activity**

The cost of the parts purchased during last quarter can be summarized as follows:

- \$587.66 Materials for the Miniaturized platform (SML)
- \$375.46 Materials for the Structure Light platform (NDEL)

#### (d) Task1. Miniaturization and upgrade of the robotic platform (SML at MSU)

In this task, MSU designs and constructs a miniaturized version of the previously tested robotic platform, as well as adjust and upgrade sections of the previous design that had some shortcomings. During this quarter, a design for this miniaturized platform was created, and a CAD drawing of the current design is shown in Figure 1. The work on this design can be categorized as:

- Design of the physical structure
- Selection of parts for miniaturization

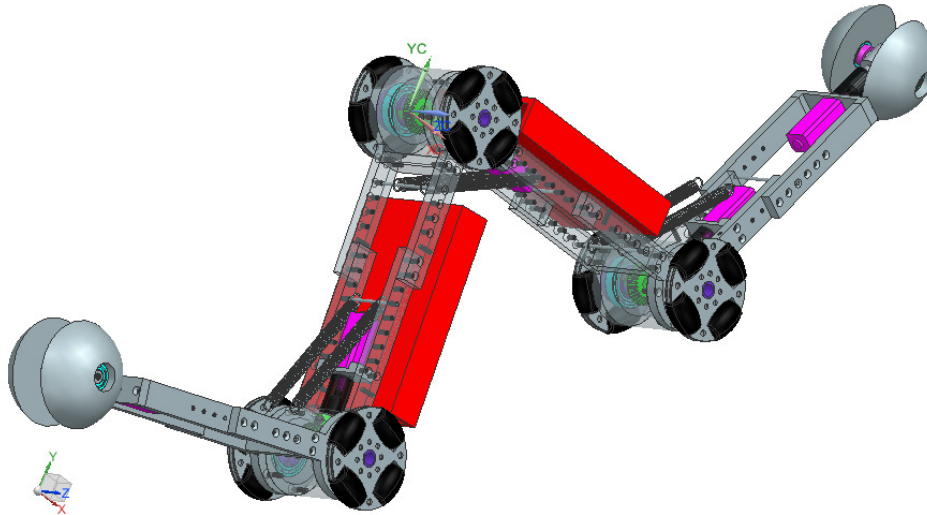


Figure 1: Miniaturized Design of the Robotic Platform

#### 1. Design of the physical structure

The design of the new robotic platform was done such that it could fit inside and operate in at least a minimum of 4-inch inner diameter pipe. The physical structure of the robot had to be redesigned in order to fit this criteria, in addition to housing the components to operate the robot.

The structure of the platform consists of three parts: the segment joints, links, and end wheels. These parts are labeled in Figure 2. The joints hold the drive for the motors and wheels required to move the robot forward and backward in the pipe. The links connect the joints and end wheels, and allow space for the electronics, motors, and batteries to be secured. The links contain multiple holes for connection, which allows for an adjustable length. This enables the robot to fit in tighter spaces if preconfigured to do so. The end wheels on both ends of the platform contain the drive system for the robot to rotate while inside a pipe. Currently a 3D printed prototype design of the platform has been made for assembly and testing purposes before a more permanent aluminum structure is created for the final design.

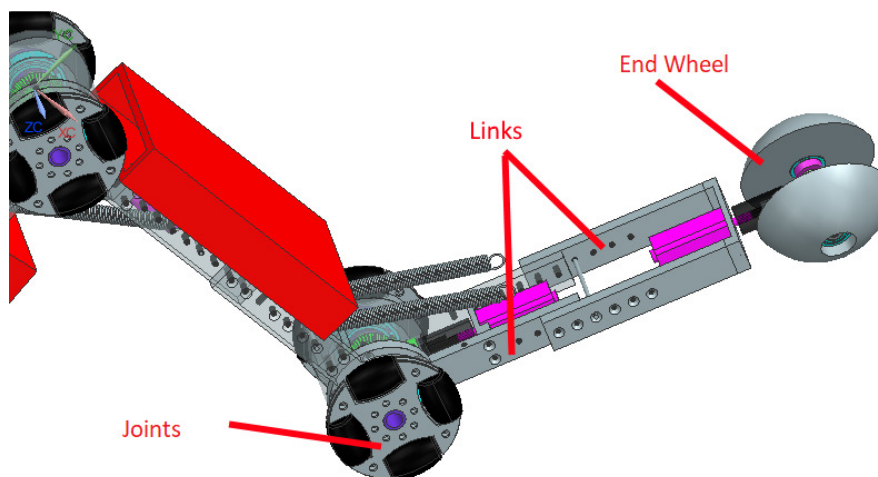


Figure 2: Labeled Design

## 2. Selection of parts for miniaturization

Various parts on the previously designed platform were too large to possibly meet size requirement of the current platform. The foremost of which was the motors, which contributed to nearly half the weight and the platform to shape around the large motors. In contrast, the much smaller motors shown in Figure 3, allow for a smaller design as well as additional space to be used for other components. The overall smaller design of the robot, as well as the lighter weight of the motors allows for the motor size reduction without a significant loss in performance. On the previous design, only two of the three joints were motorized, leaving the middle joint free rolling. Due to the smaller motor size a third motor was added for the middle joint.



Figure 3: Smaller Motor

The previous design used a torsion spring inside the joints to keep the robot pressed against the pipe for traction. The new design however, required a smaller joint size, in which the torsion spring would be difficult to fit. Instead of the torsion spring, linear springs were used outside of the joint and between the links. This allows for the size of the joints to be reduced while keeping the proper torque between the links of the platform for traction. Another component on the platform scaled down are the wheels. The previous diameter of the wheels was 60mm, and this has been reduced to 48mm to allow for the robot to fit inside a smaller pipe. The structure of the wheels remains the same, with omni-wheels for the forward drive, and hemisphere wheels for the rotation inside the pipe. Both wheels are shown in Figure 4.

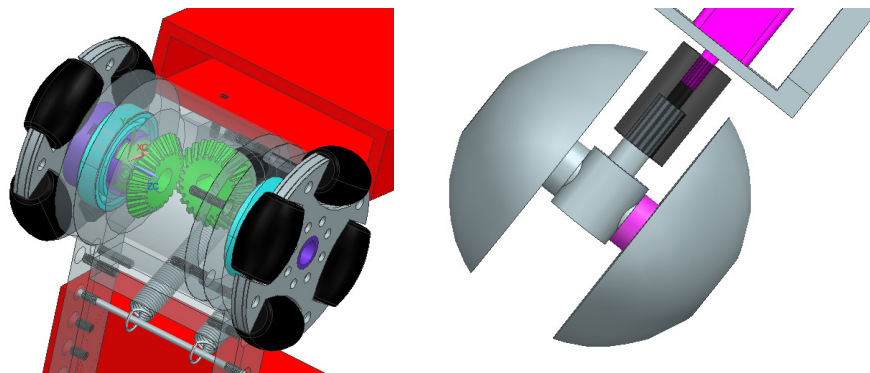


Figure 4: Omni Wheels (Left) End Wheels (Right)

The reduction in motor size allows for more components to fit inside the platform. This removes the need for a cart to be pulled by the robot carrying the batteries. This allows for the robot to operate without a tether or additional cart. The battery to be used is a 7.4V 1550mAh LiPo battery. The robot will hold 4 of these batteries as its power source. These batteries have less power capacity than the ones used in the previous design, but the smaller motors will use less power overall, likely leading to a similar operating time. The main control board for the platform will be the Raspberry Pi 4B.

## 3. Summary

This quarter MSU created a design for a miniaturized version of the previously created platform. A structure for the platform was designed to fit inside a 4-inch pipe. The motors and other components were replaced with smaller versions to reduce the size. Materials were selected to allow for untethered operation without a cart.

### (e) Task 2: Redesign and optimization of the structured light sensor (NDEL at MSU)

In this task, MSU focuses on the development and optimization of an endoscopic structured light sensor. The design and development process focuses on addressing the shortcomings that we discovered during the integration of the robotic platform. A schematic of the proposed scanning platform is shown in Figure 5. The setup consists of a structured light projection module and a camera that is placed in front of the projector. During this quarter we worked on:

1. Developing a new projection module
2. Performing sensor synchronization
3. Developing automatic calibration algorithm

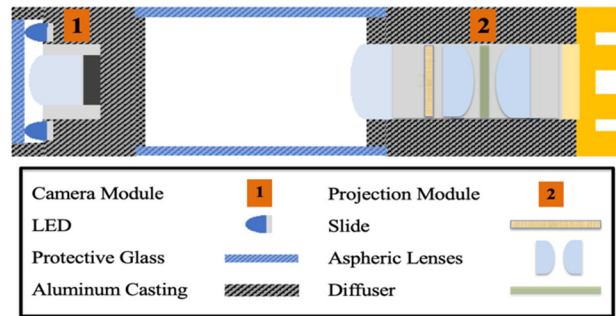


Figure 5: Schematic of the upgraded SL module

#### 1. Design of new projection module:

A new projection module was designed to:

- Improve the build quality: enhance the fabrication process to facilitate the sensor assembly, improve the error in the component's placement, and increase the rigidity of the module. The old 3D printed lens holder was exchanged with a lens tube with internal thread and retaining rings.
- Improve the sensor efficiency: a new lens system was adopted to collect the light from the light source and focus it on the transparency slide. Two aspheric condenser lenses with a light diffuser are used instead of using a single aspheric lens. Also, the previous projector lens is replaced with a 6mm projector lens with an F2.5 aperture to reduce the projection lens distortion.
- Pattern: the pattern was redesigned to reduce the code length by using a de Bruijn sequence with a code length of 2. With the three RGB colors, the total sequence length is nine ( $3^2$ ). The short code length will enable the identification of each slit individually and improve the system robustness. The schematic of the new pattern is shown in Figure 6b. The outer black boundary is only used to define the dimensions of the slide during the fabrication process and has no role in the original pattern design.

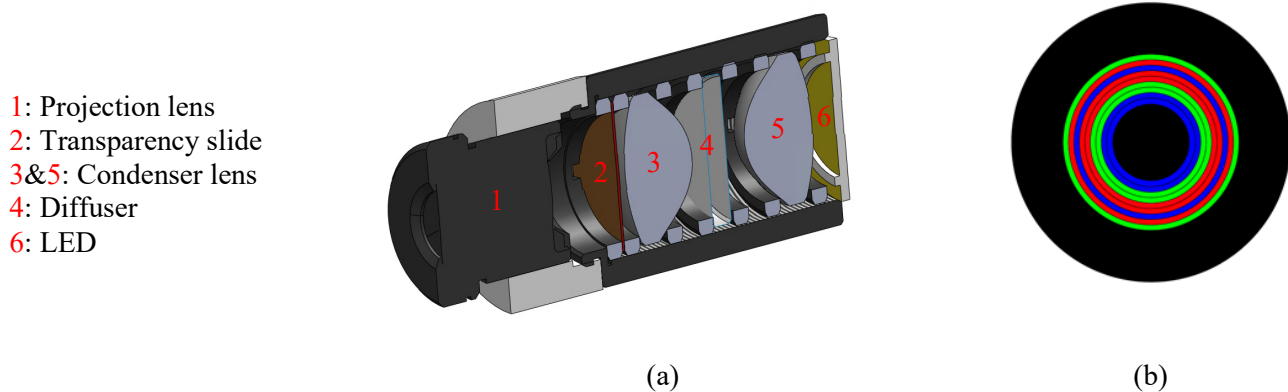


Figure 6: a) Diagram of the projection module showing its internal components, b) Colored pattern printed on the transparency slide

A 3D diagram of the designed projection module describing its main components is shown in Figure 6a, and the complete diagram of the new sensor is shown in Figure 7.

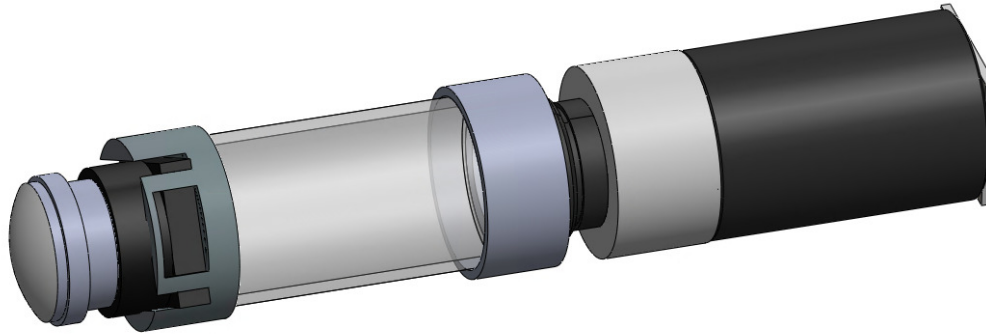


Figure 7: 3D diagram of the structured light sensor

## 2. Sensor synchronization:

In the past quarter, we reported a plan to implement synchronized acquisition between the projector and a white LED source to enable sequential acquisition from the camera with two lighting sources. The plan was to add an LED ring to the front tip of the sensor to provide extra source of illumination. In this quarter, MSU worked on implementing the synchronization procedure and integrating it with the acquisition system.

The maximum diameter of the sensor is 18mm, therefore, the ring was designed to have the same outer diameter. The internal diameter was constrained by the diameter of the lens thread (m12), therefore the ring diameter was set to 12.2 mm. This left us with relatively tight dimensions (5.8mm) for the placement of the circuitry components. Therefore, the LED was chosen to be XLAMP-XD16. The LED has a square shape and dimensions of 1.6 by 1.6 mm. Schematics of the LED geometry are shown in Figure 8. The LED also has a maximum radiant flux of 139 lm, 135 degrees viewing angle, and a forward voltage of 2.73 volts.

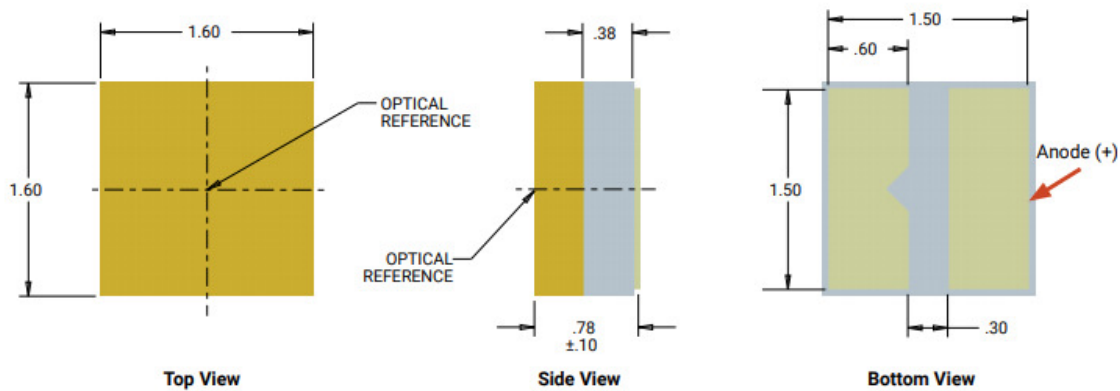


Figure 8: A schematic showing the dimensions of the XLAMP-XD16 LED

At the beginning the system was designed to work with 5.2 volts (similar to the projector LED voltage); therefore, a parallel design was followed as shown in Figure 9a. Each LED was connected in series with a 1-ohm resistor to compensate for the difference in the forward voltages. The PCB was designed and fabricated locally on FR4 boards as shown in Figure 9b and c, and d.

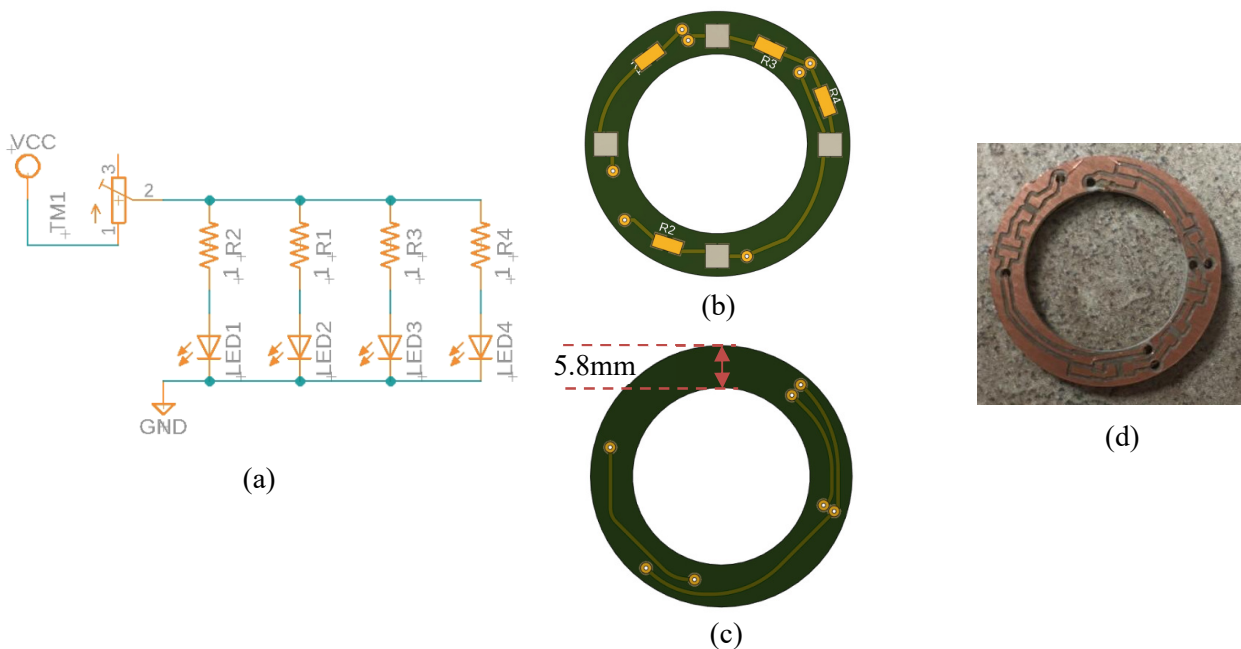


Figure 9: a) Circuit schematic, b) Top view of the PCB, c) Bottom view of the PCB, d) Fabricated PCB

After discussing with the robotic teams, it was decided to move to a 12-volt system to match the voltage of the robotic system. Therefore, the series connection was adopted as shown in Figure 10. This design further simplified the electronic circuit and reduced the number of required components. Pictures of the fabricated sensor with the attached lighting ring are shown in Figure 11a and b.

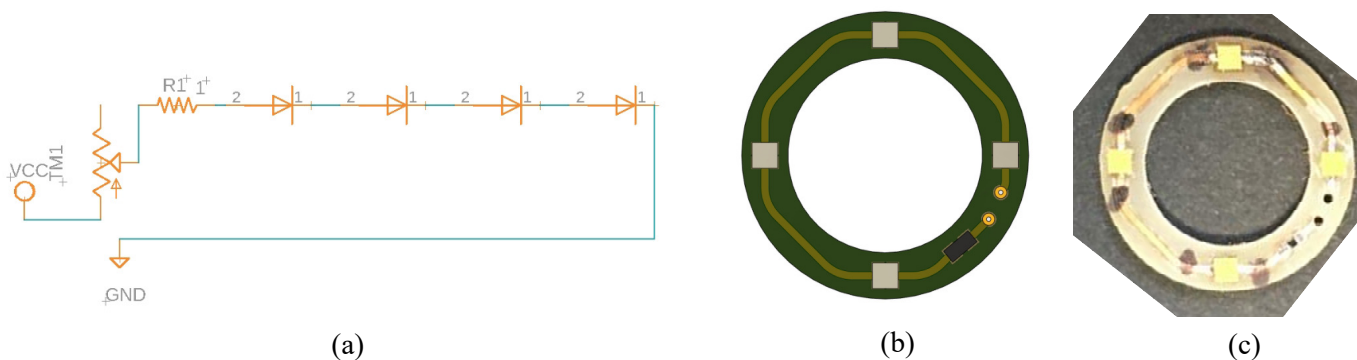


Figure 10: a) Circuit schematic, b) Top view of the PCB, c) Fabricated PCB with the soldered components



Figure 11: Pictures of the structured light sensor, a) Side view, b) Front view

The synchronization circuit schematic is shown in Figure 12. The circuit has two MOSFET switches that control the power supply to the LED and the SL projector. Both switches are controlled by the main control and acquisition board. The board is also connected to the sensor's main camera. The circuit follows the signal from the camera to trigger the circuit and change the status of the switches.

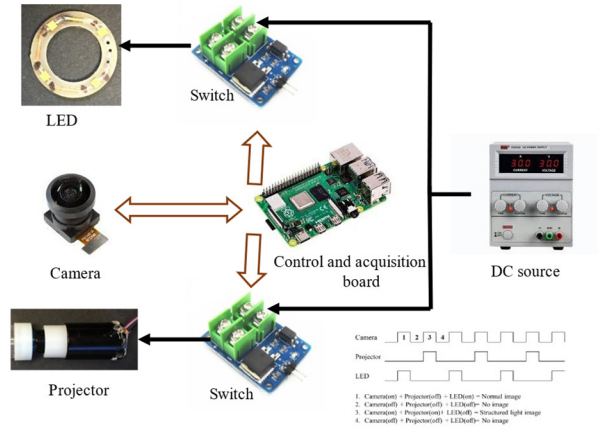


Figure 12: Schematic explaining the synchronization procedure

Direct pictures from the sensors from inspecting a 4-inch pipe are shown in Figure 13. The figure shows sequential from using the LED and the structured light projector. Future work will focus on tuning the parameters of the acquisition and synchronization circuit. This will improve the camera's white balance and ensure that both pictures have good illumination.

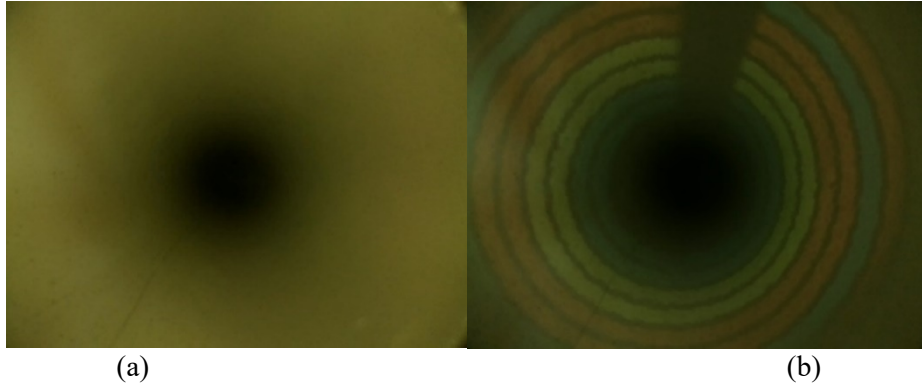


Figure 13: Sequential acquisition from inspecting 4-inch pipe, a) White LED image, b) Structured light raw image

### 3. Automatic calibration:

Accurate reconstruction of the scanned object surface requires precise determination of the scanning system parameters. The parameters include camera intrinsic parameters, angle of each projected ring from the projector, and the stereo parameters between the camera and projector. The calibration procedure starts with calibrating the camera first by following the Zhang model [1] followed by calculating the projector intrinsic parameters and the stereo parameters. The projector cannot see the external world therefore the calibrated camera is used to assist projector calibration. The process is performed in two steps. In the first step, a predefined pattern is used to obtain the orientation of the camera with respect to the calibration board. ArUco patterns were used because they can be identified even with partial obstruction of the calibration board. Once the pattern is identified, the camera orientation is calculated and the normal to the calibration board is determined. The next step is to turn on the projector and capture the colored rings by using the camera. With known camera parameters and board orientation, the 3D location of the projected rings on the board can be calculated by using the ray-plane intersection.

Each projected ring is described as a cone with a main axis ( $\vec{A}$ ), an angle ( $\theta$ ), and a vertex ( $V$ ) as shown in Figure 14. Each point that belongs to cone must satisfy:

$$\vec{A} \cdot \frac{\vec{P} - \vec{V}}{|\vec{P} - \vec{V}|} = \cos\theta$$

$\theta$  is estimated for each ring while the main axis  $\vec{A}$  and vertex  $V$  are assumed to be the same for all the rings. The values of  $\theta$  are estimated for all the rings at the same time with a constraint of  $\theta_i < \theta_{i+1}$ . A flow chart explaining the conventional calibration process is shown in Figure 14b.

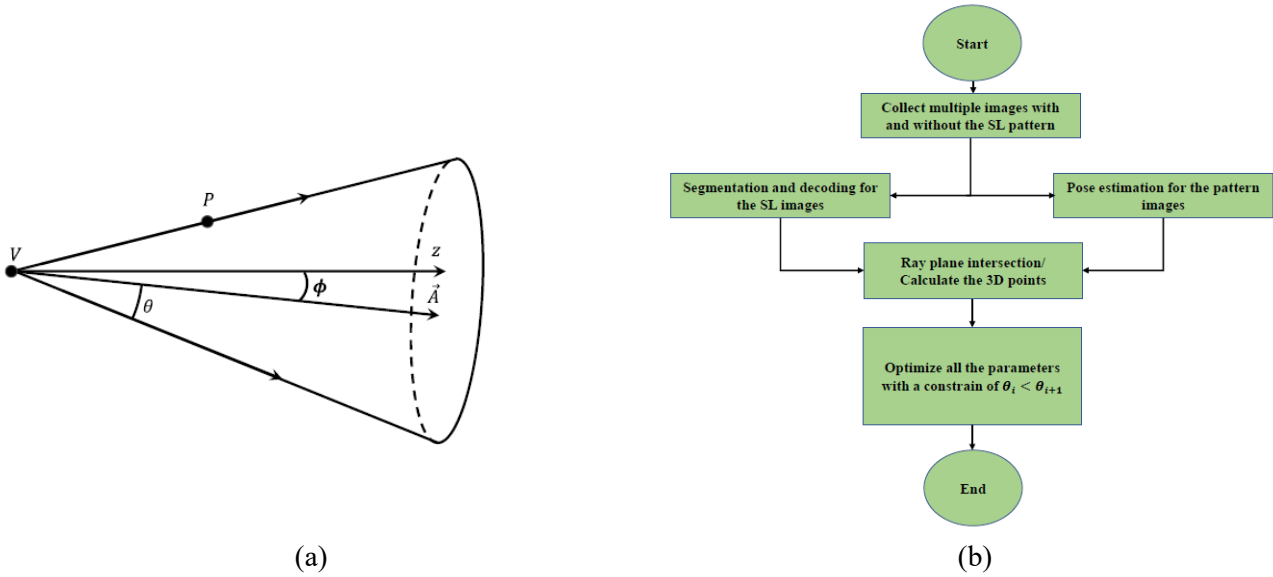


Figure 14: a) An acute cone with a main axis that is not parallel to the z-axis, b) Flow diagram of the calibration process.

In our new algorithm, we are proposing to develop an automatic calibration procure to reduce the sensor downtime and ensure accurate calibration parameters before each scan. The proposed autocalibration procedure, impose geometrical constraints to bound the fitting problem. The main concern with the calibration process is the generation of a set of 3D points to serve as an input to the calibration process. In our algorithm, we are estimating the parameters in an iterative procedure. The calibration process is explained in Figure 15. The algorithm exploits the cylindrical nature of the scanned pipes to create a set of 3D points that are used to automatically calculate the calibration parameters. The algorithm uses a cylindrical pipe with a known diameter and collects multiple images at different orientations with the help of the servo arm. The images are decoded first to create a set of 2D data. The data are reconstructed with an initial set of parameters. The reconstructed surface alignment is calculated first and the data is corrected to have a main axis that pointing in the z-direction and centered around the origin. With corrected alignment, the radius of each reconstructed point is calculated. The cost function for the fitting problem is to minimize the difference between the estimated and actual radius of the calibration pipe.

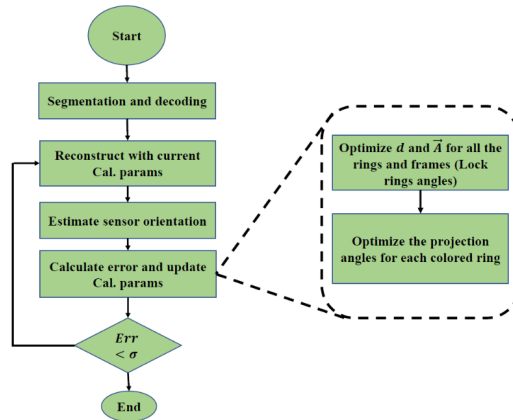


Figure 15: Automatic calibration algorithm

To test the algorithm, we created a simulation environment with POV ray that have similar geometry to the structured light sensor as shown in Figure 16a. The simulated sensor is used to scan a cylindrical pipe and the images from the simulation environment are shown in Figure 16b. The images represent a sensor at different orientations inside the pipe. These simulation results represent an ideal sensor with no camera projector misalignment. The images are fed to the calibration algorithm and the results are shown in Figure 17b. A1 to A16 represent the angles of the projected

rings (as focal length in pixels) and  $d$  represents the distance from the camera to the projector. The second column (Org) represents the actual parameters of the simulated sensors, the third column (Init.) represents the initial calibration parameters, and the last column (Est.) represents the estimated calibration parameters. Reconstruction results with the parameters in these three columns are shown in Figure 17a. The results from simulation results indicate that algorithm was able to successfully estimate the system parameters.

Applying the same algorithm to the experimental data was not successful. The reason was that the developed model didn't consider the misalignment between the projector and camera modules. The work during the next quarter will be dedicated to creating a new cost function to consider the effect of camera-projector misalignment.

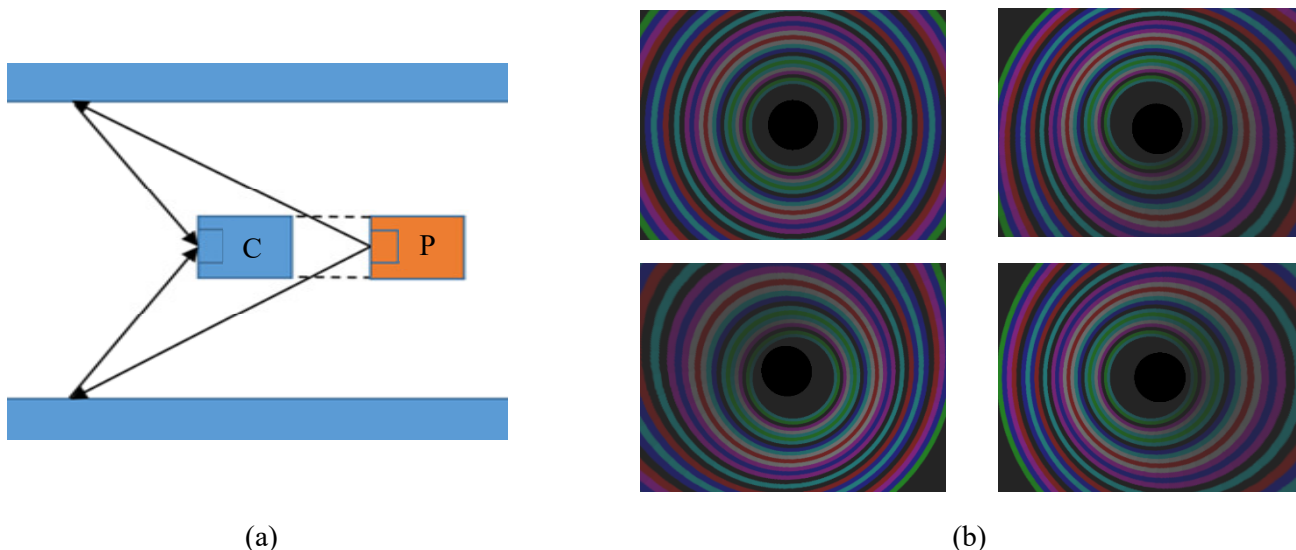


Figure 16: a) Schematic of the simulated geometry, b) Images generated for the simulation environment

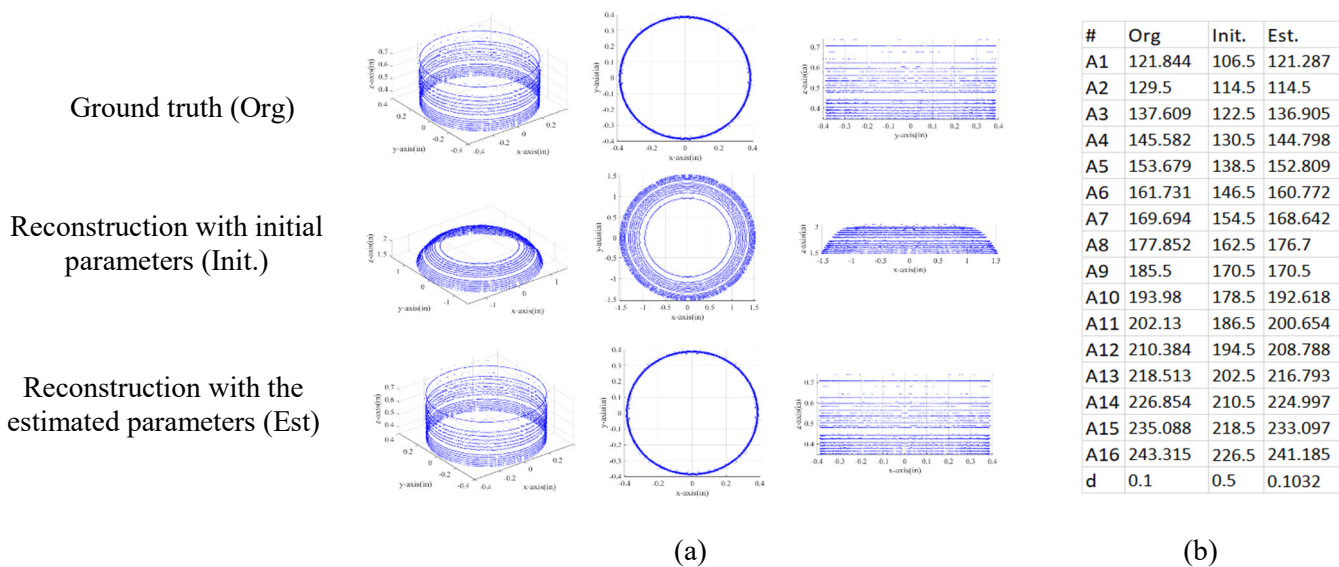


Figure 17: a) Automatic calibration with simulation data, b) Table of the calibration parameters

#### 4. Summary

In this quarter, MSU worked on implementing the work that was planned during the last quarter. A new projection module was developed to improve the build quality of the projector and improve its efficiency. The synchronization procedure was implemented, and a new lighting circle was fabricated. MSU also started the work on a new automatic calibration algorithm to estimate the projector parameters automatically without the need for user input. Initial work was successful in estimating the sensor parameters with simulation data, but further work is needed to account for camera-projector misalignment in the sensor.